Redox Biology 61 (2023) 102638

Contents lists available at ScienceDirect

Redox Biology

journal homepage: www.elsevier.com/locate/redox

Ythdf2 promotes pulmonary hypertension by suppressing Hmox1-dependent anti-inflammatory and antioxidant function in alveolar macrophages

Li Hu [a,b,1], Yanfang Yu [a,1], Yueyao Shen [a], Huijie Huang [a], Donghai Lin [a], Kang Wang [a], Youjia Yu [a], Kai Li [a], Yue Cao [a], Qiang Wang [c], Xiaoxuan Sun [c], Zhibing Qiu [d], Dong Wei [e], Bin Shen [f], Jingyu Chen [e], David Fulton [g], Yong Ji [h], Jie Wang [a,**], Feng Chen [a,b,g,i,*]

[a] Department of Forensic Medicine, Nanjing Medical University, Nanjing, China
[b] Gusu School, Nanjing Medical University, Suzhou, China
[c] Department of Rheumatology, The First Affiliated Hospital of Nanjing Medical University, Nanjing, China
[d] Department of Thoracic and Cardiovascular Surgery, Nanjing First Hospital, Nanjing Medical University, Nanjing, China
[e] Wuxi Lung Transplantation Center, Wuxi People's Hospital Affiliated with Nanjing Medical University, Wuxi, China
[f] State Key Laboratory of Reproductive Medicine, Nanjing Medical University, Nanjing, China
[g] Vascular Biology Center, Medical College of Georgia at Augusta University, Augusta, GA, USA
[h] Key Laboratory of Cardiovascular and Cerebrovascular Medicine, Key Laboratory of Targeted Intervention of Cardiovascular Disease, Collaborative Innovation Center for Cardiovascular Disease Translational Medicine, State Key Laboratory of Reproductive Medicine, Nanjing Medical University, Nanjing, China
[i] Key Laboratory of Targeted Intervention of Cardiovascular Disease, Collaborative Innovation Center for Cardiovascular Disease Translational Medicine, Nanjing Medical University, Nanjing, China

ARTICLE INFO

Keywords:
Alveolar macrophages
Oxidant stress
Inflammation
Ythdf2
Heme oxygenase 1
Pulmonary hypertension

ABSTRACT

Pulmonary hypertension (PH) is a devastating disease characterized by irreversible pulmonary vascular remodeling (PVR) that causes right ventricular failure and death. The early alternative activation of macrophages is a critical event in the development of PVR and PH, but the underlying mechanisms remain elusive. Previously we have shown that N^6-methyladenosine (m^6A) modifications of RNA contribute to phenotypic switching of pulmonary artery smooth muscle cells and PH. In the current study, we identify *Ythdf2*, an m^6A reader, as an important regulator of pulmonary inflammation and redox regulation in PH. In a mouse model of PH, the protein expression of Ythdf2 was increased in alveolar macrophages (AMs) during the early stages of hypoxia. Mice with a myeloid specific knockout of *Ythdf2* ($Ythdf2^{Lyz2\ Cre}$) were protected from PH with attenuated right ventricular hypertrophy and PVR compared to control mice and this was accompanied by decreased macrophage polarization and oxidative stress. In the absence of *Ythdf2*, heme oxygenase 1 (Hmox1) mRNA and protein expression were significantly elevated in hypoxic AMs. Mechanistically, *Ythdf2* promoted the degradation of *Hmox1* mRNA in a m^6A dependent manner. Furthermore, an inhibitor of *Hmox1* promoted macrophage alternative activation, and reversed the protection from PH seen in $Ythdf2^{Lyz2\ Cre}$ mice under hypoxic exposure. Together, our data reveal a novel mechanism linking m^6A RNA modification with changes in macrophage phenotype, inflammation and oxidative stress in PH, and identify *Hmox1* as a downstream target of *Ythdf2*, suggesting that *Ythdf2* may be a therapeutic target in PH.

1. Introduction

Pulmonary hypertension (PH) is a serious cardiopulmonary disorder that results in increased pulmonary arterial pressure, progressive right heart failure and premature death. The pathological process of PH is characterized by pulmonary vascular remodeling (PVR), which results

* Corresponding author. Key Laboratory of Targeted Intervention of Cardiovascular Disease, Collaborative Innovation Center for Cardiovascular Disease Translational Medicine, Nanjing Medical University, 101 Longmian Avenue, Jiangning District, Nanjing, Jiangsu 210029, China.
** Corresponding author.
E-mail addresses: wangjiefm@njmu.edu.cn (J. Wang), fchen@njmu.edu.cn (F. Chen).
[1] These authors contributed equally to this work.

https://doi.org/10.1016/j.redox.2023.102638
Received 19 January 2023; Received in revised form 4 February 2023; Accepted 13 February 2023
Available online 15 February 2023

from excessive proliferation of pulmonary artery smooth muscle cells (PASMCs) and pulmonary artery endothelial cells, and the abnormal accumulation of inflammatory cells [1,2]. Despite significant progress, the mechanisms triggering PVR remain incompletely understood.

Accumulating evidence suggests that lung and vascular inflammation is an important component of the pathogenesis of PH [3–5]. The infiltration of inflammatory cells and mediators have been detected in various models of PH and in PH patients [5,6]. Depletion of leukocytes by genetic approaches or immunosuppressive drugs attenuates PVR in animal models of PH [7,8]. Among the inflammatory cells implicated in PH, monocytes/macrophages have important roles associated with the pathogenesis of PH [9,10]. Macrophages have remarkable phenotypic plasticity that enables them to efficiently respond to a variety of stimuli by generating three macrophage populations that can be broadly categorized as classically activated (M1), alternatively activated (M2), and anti-inflammatory (regulatory) macrophages [11]. Of these subtypes, M2 macrophages were reported to be involved in the development of PH and other lung disorders due to their ability to promote fibrosis, injury repair and angiogenesis [12]. Furthermore, recent studies demonstrated that the recruitment of alternatively activated macrophage in the early stages of PH were critical for later PVR [13]. However, the mechanisms connecting macrophage activation with PVR remain obscure.

An increasing body of evidence suggests that posttranscriptional regulation is an important regulator of immune reactions and macrophage activation in PH [14,15]. M^6A modification is the most common modification of mRNA and has been linked to various cardiovascular diseases through the cooperation of writers, erasers and readers of this modification [16–18]. We have previously reported that m^6A modification and its effector *YTH N6-methyladenosine RNA binding protein 1 (Ythdf1)* modulate the phenotypic switching of PASMCs and contribute to PVR and PH [16]. However, our results also showed that only a small fraction of the m^6A containing transcripts (approximate 1/3) in PH lungs were recognized and bound by *Ythdf1*, which implied that other m^6A readers may contribute to the development of PH. Of the YTH domain family members, *YTH N6-methyladenosine RNA binding protein 2* (*Ythdf2*) is remarkable for promoting the degradation of m^6A-modified RNA, a function not shared with other family members [18]. Recently, *Ythdf2* was also reported to be involved in the development of PH [19,20], but the exact mechanisms by which *Ythdf2* contributes to the pathogenesis of PH remains insufficiently defined.

The RNA-binding proteins (RBPs) are highly promising therapeutic targets due to their ability to govern the fate of hundreds of transcripts at once. Although epigenetic modifications have been extensively studied in PH, the contribution of RBPs to macrophage polarization and PH remains poorly understood. As an m^6A reader, *Ythdf2* has been shown to recognize and transport m^6A-modified RNAs to a processing body and promoting their degradation [18]. The latest research also revealed that *Ythdf2* is tightly associated with inflammation and macrophage polarization [21,22]. *Ythdf2* has also been reported to be a novel diagnostic, immunotherapeutic and prognostic biomarker in various immune disorders [23,24]. The ability of *Ythdf2* to regulate macrophage inflammation and promote PVR and PH has not been demonstrated.

In our study, we investigated the expression patterns of *Ythdf2* and its molecular mechanisms in regulating inflammation, PVR and PH. We show that *Ythdf2* has an indispensable role in the alternative activation of alveolar macrophages (AMs) during the early stage of PH. Furthermore, we show, for the first time, that *heme oxygenase 1* (*Hmox1*) mRNA is modified by m^6A and is recognized by *Ythdf2*. In the progression of PH, the upregulation of Ythdf2 protein expression accelerates early macrophage activation and later hyperplasia of PASMCs by promoting *Hmox1* mRNA degradation. Specific knockout of *Ythdf2* in myeloid cells alleviated the cardiac dysfunction and PVR in PH mice by mitigating inflammatory cell infiltration and polarization and reducing the levels of oxidants in AMs. These protective effects can be reversed with *Hmox1* inhibition, suggesting that the ability of *Ythdf2* to bind m^6A marked *Hmox1* mRNA and regulate its expression is functional significant. Together, our data suggest that *Ythdf2* may be a potential therapeutic target for curbing inflammation and PVR in the pathogenesis of PH.

2. Materials and methods

All antibodies and reagents used in this study are listed in detail in Tables S1 and S2.

2.1. Human samples

Human lung sections used in this study were obtained from the Wuxi Lung Transplantation Center, Wuxi People's Hospital Affiliated with Nanjing Medical University, which has been described in detail in our previous study [16]. Human research protocols for the study were approved by the Ethics committee of Nanjing Medical University (Permit Number: 2019–452).

2.2. Animal experiments

All animal experiments were approved by the Committee on the Ethics of Animal Experiments of Nanjing Medical University (IACUC-2001008, 2004007), and all the operations and analysis were performed in a blinded manner. The $Ythdf2^{floxed}$ mice used in the present study have been previously described [25]. To generate myeloid-specific *Ythdf2* deficient mice, we crossed $Ythdf2^{floxed}$ ($Ythdf2^{wildtype}$) mice with *Lyz2-Cre* mice to generate $Ythdf2^{Lyz2\ Cre}$ mice. Male Sprague-Dawley (SD) rats (200–250g) and male wild type C57BL/6 mice aged 8–10 weeks were purchased from Animal Core Facility of Nanjing Medical University. All animals had access to standard chow and water ad libitum.

SU5416/hypoxia (Su/Hx) induced mice PH model: 8-10-week-old $Ythdf2^{wildtype}$ and $Ythdf2^{Lyz2\ Cre}$ mice received a single weekly subcutaneous injection of SU5416 (20 mg/kg body weight) or an equivalent volume of vehicle, and were then exposed to normoxic or hypoxic (10% O_2) conditions for 4 weeks. Zinc Protoporphyrin (ZnPP) treatment was carried out by i.p. injection of 40 mg/kg on days 0,1, 2, 3, 7, 14, and 21 [26,27], following PH parameters were assessed on day 28 as described below.

Hypoxic mouse model: Male 8-10-week-old male $Ythdf2^{wildtype}$ and $Ythdf2^{Lyz2\ Cre}$ mice or wildtype C57BL/6 mice were exposed to hypoxic (10% O_2) conditions for indicated days, AMs were collected from bronchoalveolar lavage fluid (BALF).

Su/Hx induced rat PH model: Male SD rats were injected s.c. with 20 mg/kg of SU5416 followed by exposure to hypoxia for 3 weeks and normoxia for another 3 weeks. Controls received the same amounts of vehicle.

Monocrotaline (MCT) induced rat PH model: Male SD rats received a single s.c. injection of 60 mg/kg MCT to induce PH, control rats were injected with the same volume of vehicle, and the animals were harvested after 4 weeks.

2.3. Echocardiography

Echocardiography was performed in $Ythdf2^{wildtype}$ and $Ythdf2^{Lyz2\ Cre}$ mice after 4 weeks of Su/Hx treatment using a Visual Sonics Vevo 2100 ultrasound machine. Velocity time integral (VTI), PA acceleration time (PAT) and PA ejection time (PET) were measured, and the results were calculated using Visual Sonics Vevo 2100 analysis software (v.1.6) with a cardiac measurement package.

2.4. Right ventricular systolic pressure (RVSP) and right ventricular hypertrophy (RVH)

After the animals were anesthetized with isoflurane, RVSP was measured by inserting a 25-gauge needle connected to a pressure transducer that was advanced into the right ventricle through the diaphragm. Following recordings of RVSP, the animals were euthanized

and the hearts were removed for subsequent analysis for RVH. The RVH index was calculated based on the following formula: [right ventricle/(left ventricle + septum)].

2.5. Histologic analysis and morphological examination

After measurement of hemodynamic parameters, lungs were inflated and harvested for downstream experiments as per our previous report [28]. Samples were fixed with 4% paraformaldehyde at 4 °C, cryoprotected using 30% sucrose solution, and embedded in optimal cutting temperature compound. Cross sections of 10 μm were prepared using a freezing microtome (CM-1950, LEICA) and stained with hematoxylin and eosin (H&E). Vascular remodeling was quantified by capturing images of H&E-stained lung tissues with an Olympus microscope and measuring medial wall thickness using Image J. Approximately 20 muscular arteries from each lung, categorized as being 25–50 μm and 50–100 μm in diameter, were outlined randomly and blindly. For evaluation the degree of muscularization, 40–60 small pulmonary arteries were assessed for each mouse, and the vessels were then categorized as non-muscular, partially muscular, or fully muscular vessels in a blinded manner.

2.6. Immunofluorescent assay

The expression of *Ythdf2* in AMs was investigated using the co-localization of Ythdf2 and F4/80 or CD68 in lung tissues. Frozen lung sections were also co-stained for proliferating cell nuclear antigen (Pcna) and actin alpha 2, smooth muscle, aorta (α-SMA) to detect proliferation of PASMCs, and co-stained for Mrc1 and α-SMA to access the degree for perivascular macrophage polarization. Nuclear 4′,6-diamidino-2-phenylindole (DAPI) was used to stain nuclei, and sections were then mounted with anti-fluorescence quench mounting medium. All fluorescent images were captured using an Olympus microscope, and quantified as described [29].

2.7. Determination of antioxidant enzymes

The levels of superoxide dismutase (SOD), glutathione (GSH), total antioxidant capacity (T-AOC) and malondialdehyde (MDA) in AMs or MH-S cells were measured using commercial assays according to the manufacturer's instructions.

2.8. Cell culture and cell transduction

A continuous cell line of murine AMs, MH-S, was procured from Procell and cultivated in RPMI 1640 containing 10% FBS at 37 °C in a 5% CO_2 atmosphere. Silencing of *Ythdf2* was achieved by transduction of a lentivirus encoding short hairpin RNA that specifically target *Ythdf2* (Tsingke Biotechnology). Stable cell lines were obtained using puromycin selection. *Ythdf2* overexpression in MH-S cell was achieved by transduction with an adenovirus encoding *Ythdf2*.

2.9. Pulmonary artery smooth muscle cells (PASMCs) proliferation assay and transwell assay

Primary mouse pulmonary artery smooth muscle cells (mPASMCs) were isolated and cultured as our previous report [16]. mPASMCs were maintained in SmGM-2 medium (Lonza) containing 5% fetal bovine serum (FBS), growth factors, and 1% penicillin-streptomycin. All mPASMCs-based experiments were performed at passage 3 to 5. For proliferation assay, mPASMCs seeded at a density of 5×10^4 were treated by serum starvation overnight, conditioned media from AMs or MH-S cells of indicated groups was applied to mPASMCs and incubated for an additional 2 days. Cell proliferation was determined by incorporation of 5-ethynyl-20-deoxyuridine (EdU) using the EdU Cell Proliferation Assay Kit (RiboBio). The EdU-positive cells were detected by an Olympus microscope, images were analyzed using the Image J analysis Software. For Transwell assay, mPASMCs pretreated with conditioned media from AMs or MH-S cells were seeded into the upper chamber of 24-well Transwell plate (Corning) with 8 μm pore filters, and serum starvation was administrated overnight before complete medium (containing 20% FBS) placed in the lower chamber. After incubation for 24 h, cells attached to the upper surface of the filter membranes were removed, and the mPASMCs that had migrated to the lower surface were stained with crystal violet. Cell migration was observed under an optical microscope and quantified.

2.10. RT-qPCR and immunoblotting

Total RNA was isolated from AMs or MH-S cells using TriZol reagent following the manufacturer's protocol and converted into cDNA using a One-Step gDNA Removal and cDNA Synthesis SuperMix (Applied Biological Materials). RT-qPCR was performed in triplicates with All-in-one™ qPCR Mix (Applied Biological Materials) in a CFX96™ Real time system (Bio-Rad). The relative amount of mRNA for each gene was normalized based on that of β-actin, and the sequences of primers used in this study are listed in Table S3. Proteins were isolated from mice lung tissues, AMs, cultured mPASMCs or MH-S cells in RIPA buffer, and Western blot analysis was performed as described previously [29].

2.11. MeRIP-qPCR and RNA immunoprecipitation (RIP)

Magna MeRIP m^6A kit (Millipore) was employed to perform m^6A RNA immunoprecipitation (MeRIP) following the manufacturer's protocol as per our previous report [16]. A sequence-based m^6A modification site predictor (SRAMP) and RNA Modification associated variants (RMVar) were used to predict the m^6A modification on the mRNA of *Hmox1* using the full transcript model and RNA secondary structure analysis [30,31]. As a result, we further confirmed the potential site by designing specific RT-PCR primers for m^6A modified *Hmox1* as follows: forward 5′-CTCACCAAAAGCACATCCAGC-3′ and reverse 5′-TACAGGCCAGTTTTGGGGCT-3′. Ythdf2-RIP peak distributions were visualized with the Integrative Genomics Viewer (IGV) and RIP assays were performed as previously described [16]. RT-qPCR was carried out to determine *Hmox1* mRNA levels in RNA samples precipitated by anti-IgG or anti-Ythdf2. The RT-qPCR primers used for Ythdf2-RIP are listed in Table S3.

2.12. Proteomic analysis

AMs isolated from $Ythdf2^{wildtype}$ and $Ythdf2^{Lyz2\ Cre}$ mice undergoing 4 days' hypoxia exposure were lysed in a Urea based lysate buffer (8 M Urea, 75 μM NaCl, 50 μM Tris-HCl, PH = 8.2). Label free proteomic analysis was carried out by the analysis and testing center of Southeast University. For each group, 7 biological replicates were analyzed to identify differentially expressed proteins by Mass spectrometry (MS). The resulting peptides were analyzed in an Orbitrap Eclipse mass spectrometer (Thermo Fisher). Each sample was analyzed on the instrument separately in a random order in discovery mode, and the acquired raw data were further analyzed as previously reported [32]. Label free quantification (LFQ) values were estimated in Proteome Discoverer using Precursor Ions Area detector node, which represent the expression levels of proteins, and duplicated protein entries with low LFQ values were removed. In addition, protein entries with a median LFQ value of 0 were also removed to exclude proteins expressed at very low levels or undetected by MS. This resulted in a trimmed list of 3191 proteins, and LFQ values from this list were used for further statistical analysis, which was performed in R-package "limma (3.38.3)" using empirical Bayesian method moderated *t*-test. P values were adjusted for subsequent multiple-testing using Benjamini-Hochberg procedure.

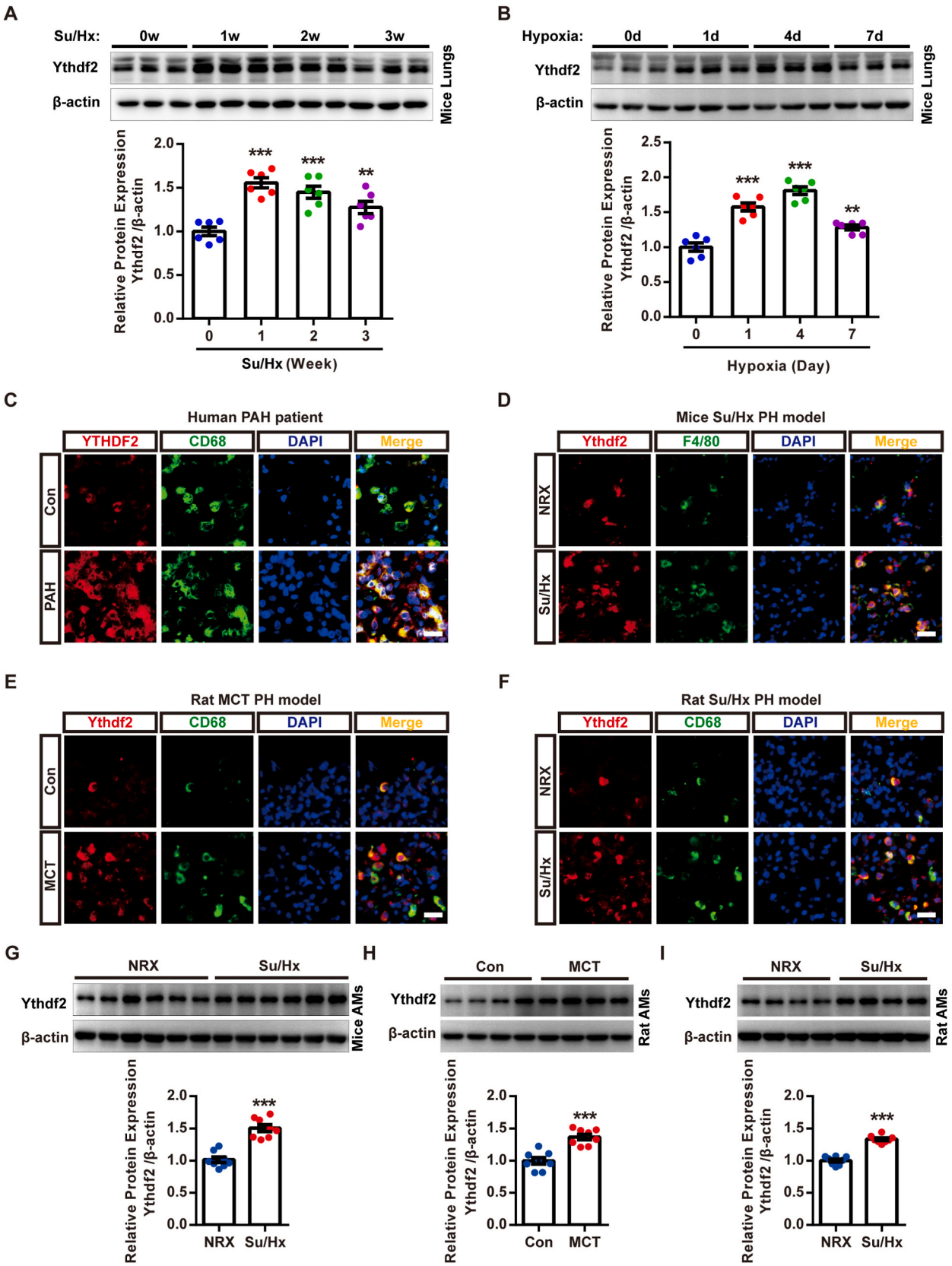

Fig. 1. Increased *Ythdf2* expression in lung macrophages are associated with PH. (A and B) Ythdf2 protein expression levels in lungs of Su/Hx-induced PH mice for indicated weeks (A) or hypoxia treated mice for indicated days (B), n = 6 mice per group. (C–F) Representative immunofluorescence of YTHDF2 (red) and CD68 (green) or F4/80 (green) in lungs of human (C), mouse (D) and rat (E and F), nuclei were counterstained with DAPI (blue), scale bars = 20 μm. (G–I) Representative immunoblots and relative densitometric analysis of Ythdf2 protein expression in AMs of mouse PH model (Su/Hx) and rat PH (MCT and Su/Hx) models normalized to β-actin, n = 8 per group. The data are shown as mean ± SE; **P < 0.01 and ***P < 0.001. Su/Hx = SU5416/hypoxia, AMs = alveolar macrophages. (For interpretation of the references to colour in this figure legend, the reader is referred to the Web version of this article.)

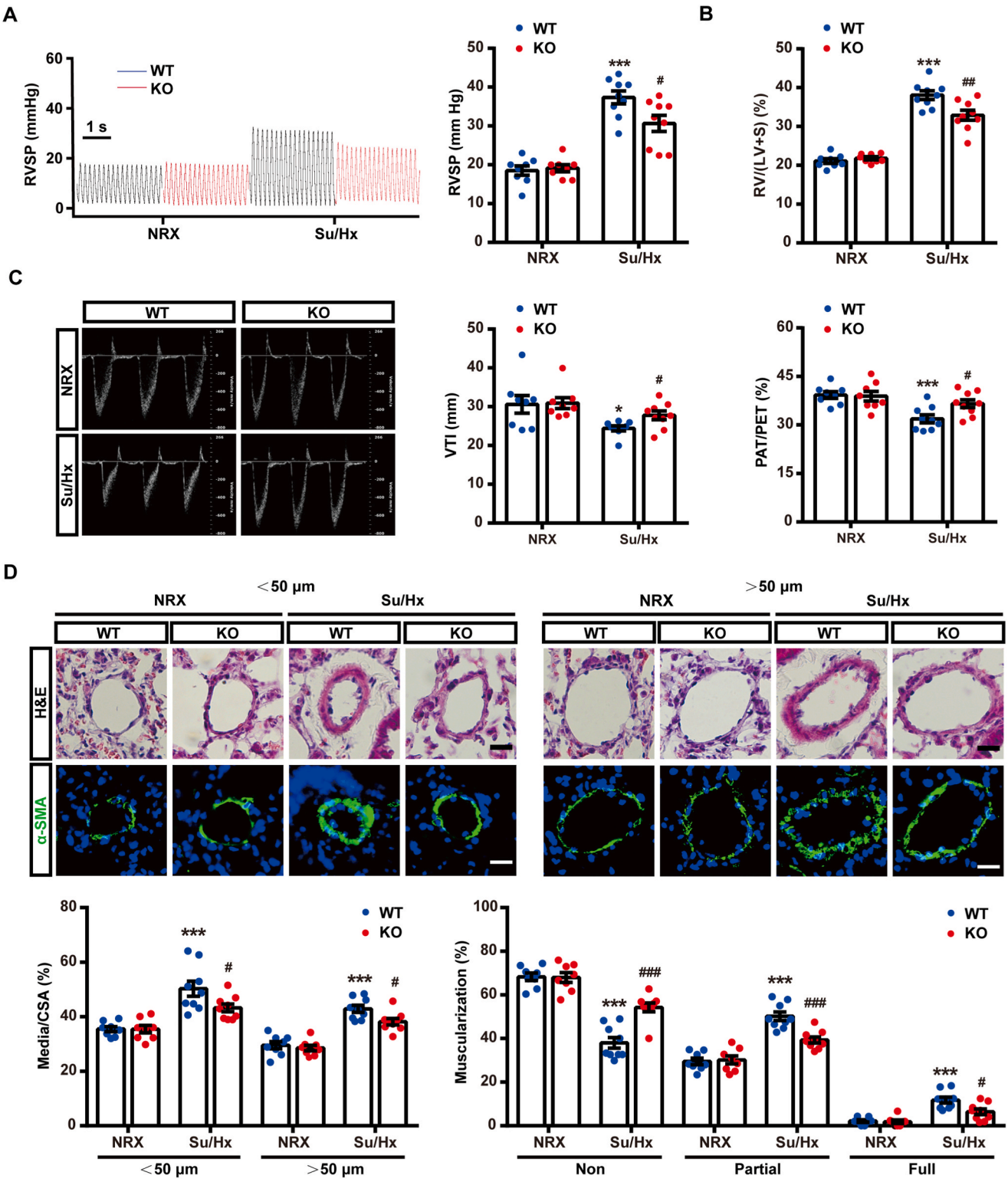

Fig. 2. Myeloid cell type-specific *Ythdf2* deletion prevents development of Su/Hx induced PH in mice. (A) Representative images and quantification of the right ventricular (RV) systolic pressure (RVSP) waves, (B) the ratio of RV to left ventricular (LV) wall plus septum (S) (RV/[LV + S]), (C) representative echocardiographic images and quantification of the velocity time integral (VTI), and the ratio of pulmonary artery accelerate time to ejection time (PAT/PET) in WT and KO mice after 4 weeks of normoxia or Su/Hx treatment. (D) Top, H&E staining and α-SMA (green) immunostaining representative images of lung sections are shown, nuclei were counterstained with DAPI (blue), scale bars = 20 μm. Bottom, quantification of vascular medial thickness and proportion of non, partially, or fully muscularized pulmonary arteries. In A-D, n = 8–9 mice per group. The data are shown as mean ± SE; *P < 0.05, ***P < 0.001 vs WT (NRX) group; $^{\#}$P < 0.05, $^{\#\#}$P < 0.01, $^{\#\#\#}$P < 0.001 vs WT (Su/Hx) group. H&E = Hematoxylin and eosin; CSA = cross-sectional area; Su/Hx = SU5416/hypoxia; NRX = normoxia; WT=*Ythdf2*^{wildtype}; KO=*Ythdf2*$^{Lyz2\ Cre}$. (For interpretation of the references to colour in this figure legend, the reader is referred to the Web version of this article.)

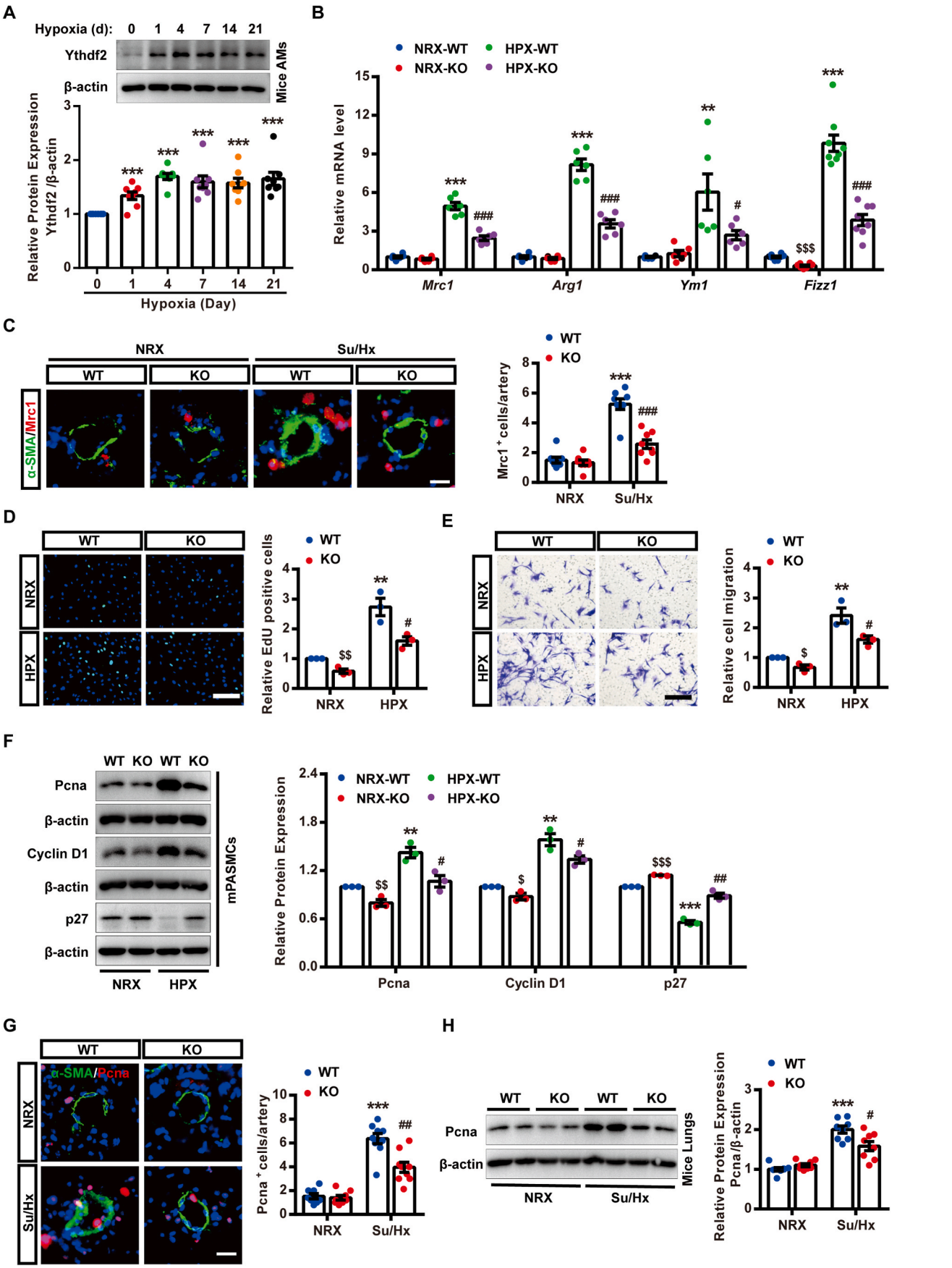

(caption on next page)

Fig. 3. Myeloid *Ythdf2* deficiency leads to altered macrophages phenotype and decreased PASMCs proliferation. (A) Ythdf2 protein expression in AMs of hypoxia treated mice for indicated days, n = 8 mice per group. (B) Relative mRNA levels of *Mrc1*, Arg*1*, *Ym1* and *Fizz1* in AMs of WT and KO mice after 4 days of normoxia or hypoxia treatment, n = 6–8 mice per group. (C) Immunofluorescence staining of lung samples from WT and KO mice for α-SMA (green) and Mrc1 (red) after 4 weeks of normoxia or Su/Hx treatment, and $Mrc1^+$ cells were quantified in each pulmonary arteries, scale bars = 20 μm, n = 8–9 mice per group. (D) Representative images and quantification of EdU (green) staining, (E) Transwell assay, and (F) representative immunoblots and relative densitometric analysis of Pcna, Cyclin D1 and p27 protein expression levels in mPASMCs exposed to conditioned media from AMs of WT and KO mice under normoxic or hypoxic conditions treated for 4 days. For D-F, scale bars = 200 μm, and results are representative of 3 separate experiments. (G) Representative immunofluorescence images of lung sections stained with Pcna (red) and α-SMA (green) with cell nuclei labeled with DAPI, scale bars = 20 μm, n = 8–9 mice per group. (H) Protein levels of Pcna in mice lung tissues, n = 8 mice per group. The data are shown as mean ± SE; $^{**}P < 0.01$, $^{***}P < 0.001$, $^{\$}P < 0.05$, $^{\$\$}P < 0.01$, $^{\$\$\$}P < 0.001$ vs WT (NRX) group; $^{\#}P < 0.05$, $^{\#\#}P < 0.01$, $^{\#\#\#}P < 0.001$ vs WT (HPX or Su/Hx) group. AMs = alveolar macrophages; HPX = hypoxia; Su/Hx = SU5416/hypoxia; WT=$Ythdf2^{wildtype}$; KO=$Ythdf2^{Lyz2\ Cre}$; mPASMCs = mouse pulmonary artery smooth muscle cells. (For interpretation of the references to colour in this figure legend, the reader is referred to the Web version of this article.)

2.13. Statistical analysis

Graphs and statistical analysis were completed using GraphPad Prism version 5.0 for Windows. The mean ± SE was calculated for all experimental data, and the *in vitro* data are analyzed with at least 3 separate experimental repeats. Statistical significance between 2 groups was calculated using 2-tailed Student *t*-test for parametric variables and Mann-Whitney *U* test for nonparametric variables. One-way ANOVA with Tukey post hoc test was used for comparisons between multiple groups. A value of $p < 0.05$ was considered to be statistically significant.

3. Results

3.1. Ythdf2 is significantly enriched in pulmonary macrophages of PH

To investigate the role of *Ythdf2* in PH, we examined the expression of Ythdf2 protein in the lung tissues of Su/Hx or hypoxia treated mice during the progression of PH. As shown in Fig. 1A and B, Ythdf2 protein expression was significantly increased in the earlier period of PH, suggesting *Ythdf2* may be related to pulmonary inflammation in PH. Moreover, immunofluorescence (IF) staining revealed that *Ythdf2* was obviously enriched in macrophages of lung sections from pulmonary arterial hypertension (PAH) patients, Su/Hx induced PH mice, as well as MCT or Su/Hx induced PH rats (Fig. 1 C-F). As a result, elevated Ythdf2 protein expression was observed in AMs isolated from BALF of various PH animal models (Fig. 1 G-I). These data indicated that up-regulated Ythdf2 expression of pulmonary macrophages were probably involved in the pathophysiological process of PH.

3.2. Mice with a specific deficiency of Ythdf2 in myeloid cells are protected from Su/Hx-induced PH

To determine whether *Ythdf2* is functionally important in PH, we generated mice with *Ythdf2* deficiency in myeloid cells by breeding $Ythdf2^{floxed}$ mice with $Lyz2^{Cre}$ transgenic mice. Compared with $Ythdf2^{wildtype}$ mice, decreased Ythdf2 protein expression was observed in AMs and bone marrow derived macrophage (BMDM) of $Ythdf2^{Lyz2\ Cre}$ mice (Figs. S1A–C), while Ythdf1 protein expression showed no significant difference either in the lungs or in the AMs between $Ythdf2^{wildtype}$ and $Ythdf2^{Lyz2\ Cre}$ mice (Figs. S2A and B). To evaluate the effect of *Ythdf2* on macrophages in PH pathogenesis, both $Ythdf2^{wildtype}$ and $Ythdf2^{Lyz2\ Cre}$ mice were subjected to Su/Hx treatment for 4 weeks to develop PH. The data showed that RVSP and RV/(LV + S) were significantly increased in $Ythdf2^{wildtype}$ mice treated with Su/Hx, while myeloid-specific *Ythdf2*-deficient mice were protected from Su/Hx-induced increases in RVSP and RV/(LV + S) (Fig. 2A and B). Similarly, improved echocardiographic parameters were detected in $Ythdf2^{Lyz2\ Cre}$ mice, suggesting mice lacking *Ythdf2* in myeloid cells can alleviate cardiac dysfunction in mice under Su/Hx exposure (Fig. 2C). PVR is the primary histopathologic characteristics of PH [1,2]. H&E staining showed that myeloid *Ythdf2* deficiency attenuated the occlusion and muscularization of pulmonary arterioles in Su/Hx induced PH mice. Similar results were also obtained by the α-SMA IF staining (Fig. 2D). Thus, these data support the hypothesis that *Ythdf2* deficiency in myeloid cells ameliorated PVR and cardiac dysfunction of PH mice.

3.3. Myeloid Ythdf2 deficiency decreases the early alternative activation of macrophages and attenuates the subsequent PVR of PH

To further investigate the role of *Ythdf2* in macrophages of PH lungs, we examined the expression of Ythdf2 protein in AMs at different stages of PH development. As a result, increased Ythdf2 protein was detected in AMs at the first day of hypoxia. During the progression of PH, the Ythdf2 protein peaked on day 4 and remained elevated until day 21 after hypoxia exposure (Fig. 3A). M2 polarization of AMs induced by hypoxia is a cell autonomous phenomenon [13]. The phenotypic switching of macrophages occurred within the first 4 days of hypoxia, thus we hypothesized that the upregulation of *Ythdf2* in this key period may mediate the macrophage activation and polarization. Both $Ythdf2^{wildtype}$ and $Ythdf2^{Lyz2\ Cre}$ mice were exposed to hypoxia for 4 days to demonstrate the potential effect of *Ythdf2* on M2 polarization. RT-qPCR analysis identified a significant induction of well-defined markers of M2 macrophages in AMs from hypoxic $Ythdf2^{wildtype}$ mice, including *mannose receptor, C type lectin-1 (Mrc1), arginase-1 (*Arg*1), chitinase-3-like-3 (Ym1)*, and *found in inflammatory zone-1 (Fizz1)*. *Ythdf2* deficiency in myeloid cells downregulated whereas *Ythdf2* overexpression in MH-S cells upregulated the expression of these signature genes (Fig. 3B and Fig. S3A). Interestingly, the mRNA levels of *interleukin 6 (Il6)* and *chemokine (C–C motif) ligand 2 (Ccl2)* were also decreased in the lungs of $Ythdf2^{Lyz2\ Cre}$ mice after hypoxia for 4 days, which have been reported as noncanonical inducers of M2 polarization (Fig. S4A) [33–35]. More importantly, the number of $Mrc1^+$ macrophage was significantly decreased in the lungs of Su/Hx induced $Ythdf2^{Lyz2\ Cre}$ mice as compared to $Ythdf2^{wildtype}$ mice (Fig. 3C). Our results indicated that myeloid deficiency of *Ythdf2* attenuated macrophage alternative activation at the early stage of hypoxia in PH.

It has been reported that M2 macrophages contribute to the proliferation of PASMCs in PH development [3,36,37]. Given that myeloid *Ythdf2* deficiency decreased PVR in Su/Hx-induced PH mice, we next evaluated the effect of myeloid *Ythdf2* deficiency on PASMCs proliferation both in *vitro* and *in vivo*. Conditioned media (CM) derived from AMs isolated from $Ythdf2^{wildtype}$ and $Ythdf2^{Lyz2\ Cre}$ mice exposed to hypoxia for 4 days, as well as their normoxic controls were collected and incubated with mPASMCs. The EdU assay and Transwell assay showed that PASMCs proliferation and migration were increased following incubating with CM from hypoxic $Ythdf2^{wildtype}$ AMs compared with those from normoxic AMs. However, CM from $Ythdf2^{Lyz2\ Cre}$ mice AMs isolated after hypoxia exposure attenuated the proliferation and migration of PASMCs (Fig. 3D and E). Consistently, Western blot (WB) analysis demonstrated that upregulation of Pcna and Cyclin D1, along with downregulation of p27 were also detected in mPASMCs incubated with CM from hypoxic $Ythdf2^{wildtype}$ mice AMs, while *Ythdf2* myeloid deficiency abrogated these observations (Fig. 3F). In contrast, CM from *Ythdf2* overexpressed MH-S cells after hypoxia exposure aggravated PASMCs proliferation and migration *in vitro* (Figs. S3B–D). Meanwhile, we also investigated the direct effect of myeloid *Ythdf2* deficiency on

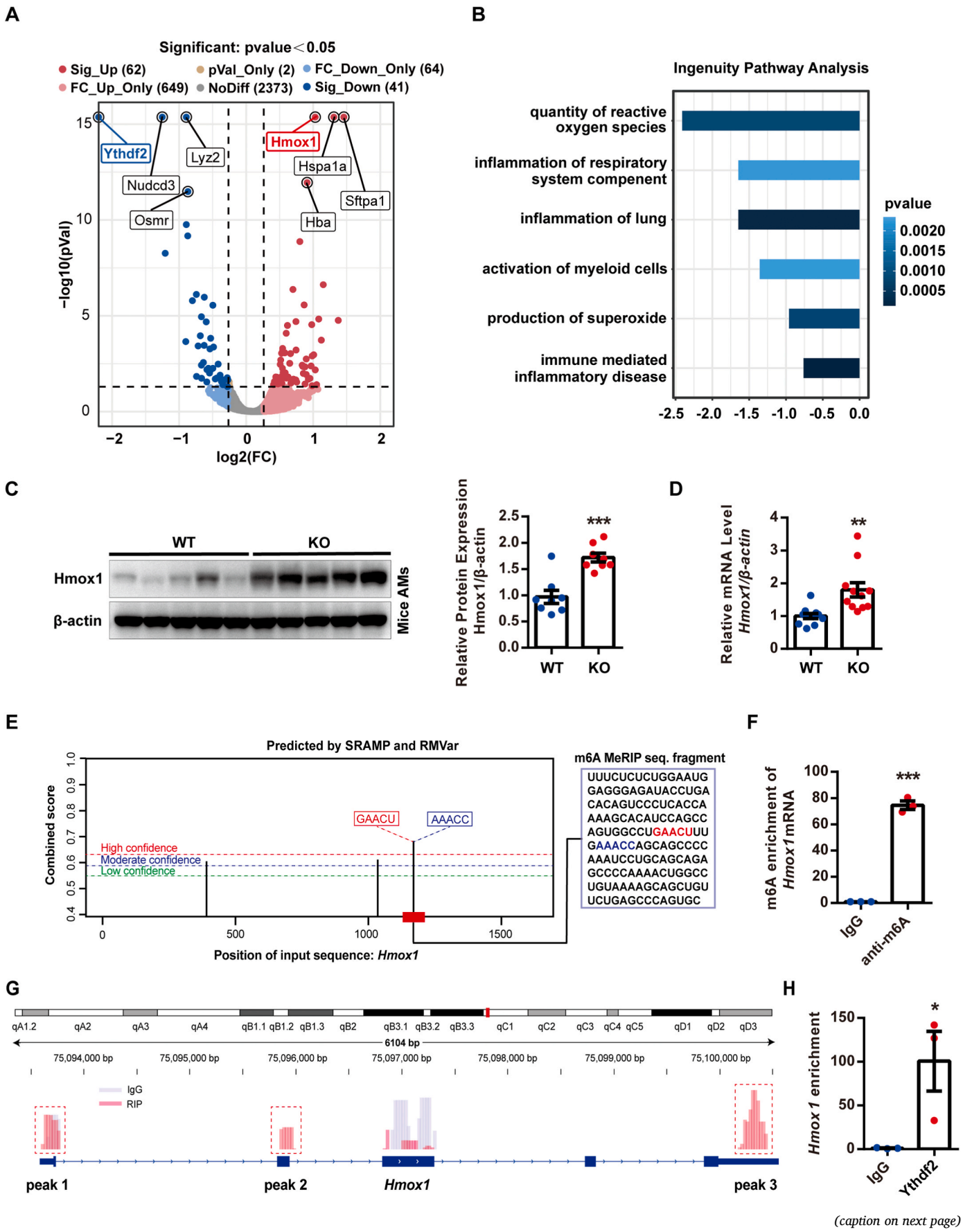

(caption on next page)

Fig. 4. *Hmox1* is a target of m^{6}A modification and *Ythdf2* in alveolar macrophages. (A) The volcano plot showing the differentially expressed proteins in AMs of WT and KO mice after 4 days of hypoxia treatment, n = 7 mice per group (significance cutoff $P < 0.05$). (B) Ingenuity Pathway Analysis of the differentially expressed proteins in (A). (C) Protein levels, (D) and mRNA levels of *Hmox1* in AMs of WT and KO mice after 4 days of hypoxia treatment, n = 8–11 mice per group. (E) The potential m^{6}A sites of *Hmox1* were predicted by SRAMP (Color lines of green, blue, and red respectively represent low, moderate, high confidence) and RMVar. (F) MeRIP-qPCR was applied to detect the m^{6}A enrichment of *Hmox1* mRNA in MH-S cell line. (G) IGV analysis for Ythdf2 binding site of *Hmox1* mRNA. (H) RIP analysis of Ythdf2 protein binding to *Hmox1* mRNA in MH-S cell line. For E-H, results are representative of 3 separate experiments. The data are shown as mean ± SE; *$P < 0.05$, **$P < 0.01$, ***$P < 0.001$. AMs = alveolar macrophages; MeRIP = m^{6}A RNA immunoprecipitation; SRAMP=Sequence-based RNA Adenosine Methylation site Predictor; RMVar = RNA Modification associated variants; WT=*Ythdf2*^{wildtype}; KO=*Ythdf2*$^{Lyz2\ Cre}$. (For interpretation of the references to colour in this figure legend, the reader is referred to the Web version of this article.)

PASMCs proliferation *in vivo*. Double-staining of proliferation marker Pcna and α-SMA showed a marked decrease in the number of positive cells for Pcna in lungs of Su/Hx-treated *Ythdf2*$^{Lyz2\ Cre}$ mice as compared with *Ythdf2*^{wildtype} mice (Fig. 3G). Correspondingly, the Pcna protein expression level was dramatically decreased in the lungs of *Ythdf2*$^{Lyz2\ Cre}$ mice compared with that of *Ythdf2*^{wildtype} mice after Su/Hx treatment (Fig. 3H). The above data indicated that altered macrophage polarization caused by myeloid *Ythdf2* deficiency can alleviate PASMCs proliferation and improve the later PVR in the pathogenesis of PH.

3.4. Heme oxygenase 1 is identified as a target of m^{6}A modification and Ythdf2 in macrophages

In order to elucidate the molecular mechanism of *Ythdf2* in early polarization of macrophages in the PH pathogenesis, proteomic analysis was performed in AMs from mice after 4 days of hypoxic treatment. The differentially expressed proteins between *Ythdf2*^{wildtype} and *Ythdf2*$^{Lyz2\ Cre}$ AMs were visualized as a volcano plot and a heatmap (Fig. 4A and Fig. S5A). Ingenuity Pathway Analysis (IPA) software was employed to further characterize the biological functions and the pathways involved in the regulation of the identified 103 differentially expressed proteins. The results showed that several pathways involved in inflammatory response and oxidative stress were significantly suppressed in *Ythdf2*$^{Lyz2\ Cre}$ AMs compared to *Ythdf2*^{wildtype} AMs (Fig. 4B). Redox regulation has been reported to play important roles in immunomodulation, and excessive production of reactive oxygen species (ROS) can trigger inflammation response [38]. Meanwhile, oxidant dysfunction was also associated with the pathogenesis of PH. The major function of *Ythdf2* is mediating target mRNAs degradation by recognizing the m^{6}A containing RNAs. Thus, the upregulated proteins in *Ythdf2*$^{Lyz2\ Cre}$ AMs as compared to *Ythdf2*^{wildtype} AMs were prioritized to be considered as the potential downstream target of *Ythdf2*. Based on the critical role of Heme oxygenase 1 (Hmox1) in anti-inflammatory and antioxidant properties in cardiovascular diseases, we selected to focus on *Hmox1* as a downstream target gene of *Ythdf2* in this study. As a result, Hmox1 was significantly increased in AMs from *Ythdf2*$^{Lyz2\ Cre}$ mice compared to *Ythdf2*^{wildtype} mice, and the protein and RNA expression levels of Hmox1 were further verified by WB and RT-qPCR (Fig. 4C and D). As a rate-limiting enzyme of heme degradation, *Hmox1* can convert cellular heme to carbon monoxide (CO), Fe^{2+} and biliverdin, thus play crucial roles in anti-inflammation, anti-oxidation, anti-apoptosis, anti--proliferation and anti-thrombosis in various vascular cells [39,40]. Meanwhile, *Hmox1* and its catalytic products have also been reported to be involved in the pathogenesis of PH [13,41–43]. However, it is unclear whether *Hmox1* can be modified and regulated by m^{6}A modification and *Ythdf2*.

Hence here in our study, sequence-based RNA adenosine methylation site predictor (SRAMP, http://www.cuilab.cn/sramp) [30], an online m^{6}A sites prediction tool, was employed to screen for the potential m^{6}A sites of *Hmox1* mRNA. As shown in Fig. 4E, two m^{6}A sites in coding region sequence of *Hmox1* mRNA were identified, and the motif was well-matched with RRACH. We further confirmed whether the *Hmox1* mRNA could be modified with m^{6}A in AMs. As a result, MeRIP-qPCR suggested that m^{6}A modification was significantly enriched in *Hmox1* mRNA compared to the IgG negative control in MH-S cells (Fig. 4F). Meanwhile, IGV plots demonstrated that there were three *Ythdf2* binding sites in *Hmox1* mRNA (Fig. 4G), and the following RIP assay also confirmed that *Hmox1* mRNA can be recognized and bound by Ythdf2 in mouse AMs (Fig. 4H). Collectively, these observations highlight that *Hmox1* is a pivotal downstream target of m^{6}A modification and *Ythdf2* in AMs during the progression of PH development.

3.5. Ythdf2 promotes inflammation and oxidative stress of alveolar macrophages in the development of PH by degrading Hmox1 mRNA

Next, we examined the *Hmox1* expression pattern in PH condition using WB. The protein expression level of Hmox1 was much lower in AMs isolated from Su/Hx induced-PH mice than their control mice, while its expression was slightly downregulated in lung tissues (Figs. S6A and B). Notably, significantly downregulation of Hmox1 protein was found in AMs from mice after hypoxia for 1 days (Fig. 5A), which corresponded to the upregulation of Ythdf2 protein. In line with its protein expression, the mRNA levels of *Hmox1* were also remarkably decreased in AMs form mice treated with short-term hypoxia and Su/Hx (Fig. 5B and Fig. S6C). In addition, Hmox1 level was also evaluated by enzyme linked immunosorbent assay (ELISA) assay, and the results showed that elevated expression of Hmox1 were examined in BALF and CM from hypoxic *Ythdf2*$^{Lyz2\ Cre}$ mice compared to those from their controls (Fig. 5C and D), which provides a basis for anti-inflammation and antioxidation upon *Ythdf2* deficiency. As shown in Fig. 5E–H, the increased levels of SOD, GSH, T-AOC and decreased concentration of MDA (the end product of lipid peroxidation) were detected in AMs of hypoxic *Ythdf2*$^{Lyz2\ Cre}$ mice as compared with those of *Ythdf2*^{wildtype} mice, indicating myeloid specific *Ythdf2* deficiency attenuated the oxidative stress in hypoxic AMs. Further analysis showed that *Ythdf2* overexpression in MH-S cells exacerbated oxidative stress under hypoxia condition (Fig. S3E). Meanwhile, the results of RT-qPCR showed that the mRNA levels of inflammatory cytokines and growth factors were decreased in AMs from *Ythdf2*$^{Lyz2\ Cre}$ mice compared with those of *Ythdf2*^{wildtype} mice with Su/Hx treated (Fig. S7A). Moreover, *Hmox1* and CO were reported to promote the expression of *interleukin 10* (*Il10*) in AMs, a well-documented anti-inflammatory mediator. Consistent with these findings, we found markedly higher level of *Il10* in AMs from *Ythdf2*$^{Lyz2\ Cre}$ mice after hypoxia for 4 days, which is accompanied with the upregulation of Hmox1 protein (Fig. 5I). The aforementioned results suggested that myeloid *Ythdf2* deficiency reduced the inflammation and oxidative stress in AMs of PH mice through upregulating the protein expression of Hmox1.

As previous work reported, *Ythdf2* could induce the target mRNAs degradation by reading the m^{6}A modification sites [17,18]. We further investigated if *Ythdf2* can regulate the mRNA stability of *Hmox1*. We established stable *Ythdf2* knockdown MH-S cells using lentiviral shRNAs. In MH-S cells with *Ythdf2* knockdown, protein expression and mRNA levels of *Hmox1* were significantly increased (Fig. 5J and K), which in keeping with the results of AMs isolated from *Ythdf2*$^{Lyz2\ Cre}$ mice. Next, RNA stability was investigated by suppressing new RNA synthesis in MH-S cell with actinomycin D (ActD). RT-qPCR analysis revealed that the stability of *Hmox1* mRNA was markedly enhanced in MH-S cells with Ythdf2 knockdown (Fig. 5L). Moreover, in *Ythdf2* overexpressing MH-S cells, there was a significant decrease in Hmox1 protein and mRNA expression (Fig. 5M and N), which further confirmed the effect of *Ythdf2* on *Hmox1* mRNA degradation. Overall, the above

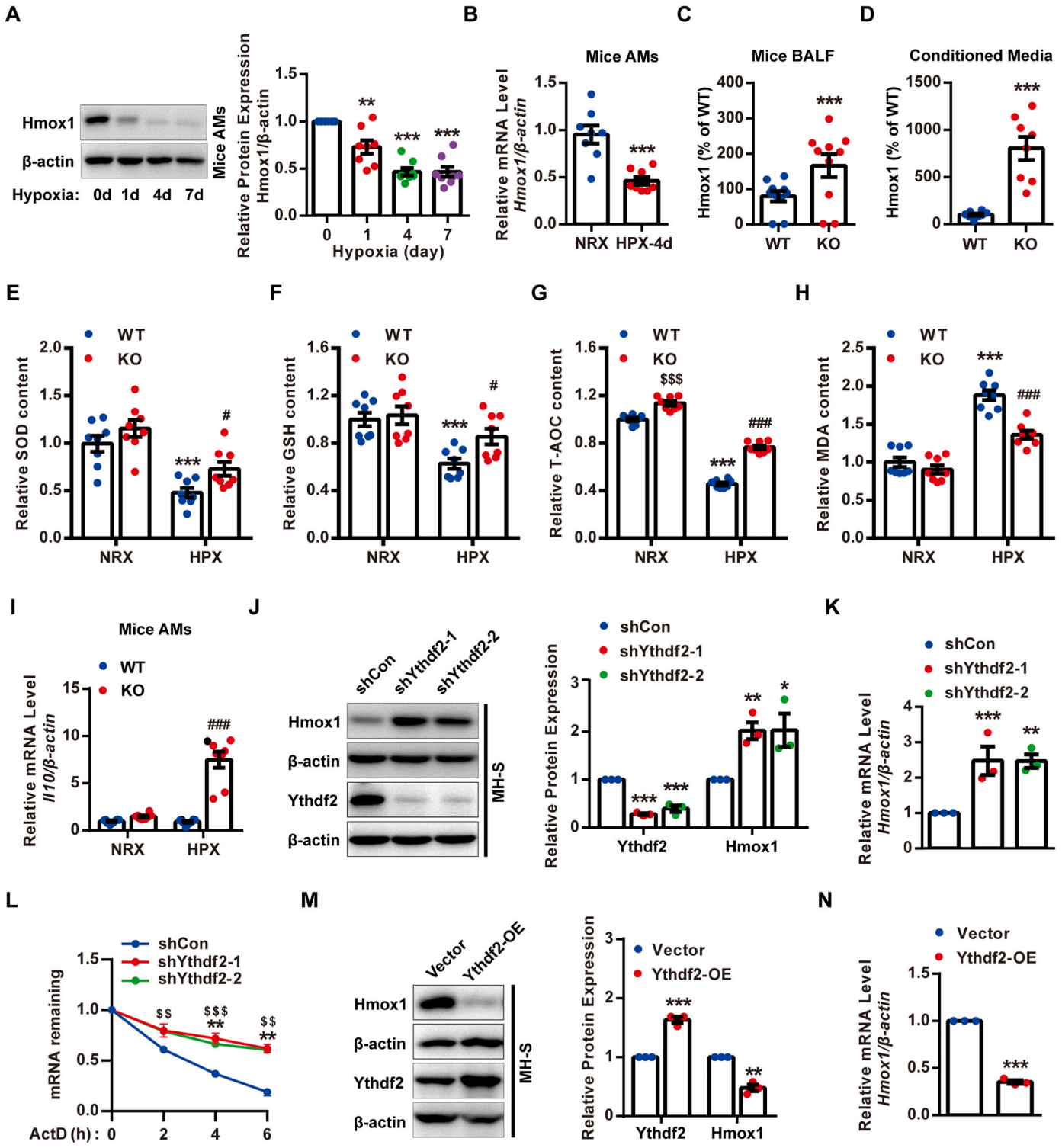

Fig. 5. *Ythdf2* promotes inflammation and oxidative stress by increasing *Hmox1* mRNA degradation. (A) Hmox1 protein expression in AMs from hypoxia treated mice for indicated days. (B) The mRNA levels of *Hmox1* in AMs isolated from control and hypoxic mice treated for 4 days. (C) ELISA-determined protein concentrations of Hmox1 in the BALF, (D) conditioned media of AMs. (E–I) The content of (E) SOD, (F) GSH, (G) T-AOC and (H) MDA, (I) and mRNA levels of *Il10* in AMs from WT and KO mice exposed to normoxia or hypoxia for 4 days. (J) Hmox1 and Ythdf2 protein levels, (K) and mRNA levels in shControl or shYthdf2-lentivirus infected MH-S cells. (L) RT-qPCR analysis of the decay rate of *Hmox1* mRNA at the indicated times after Actinomycin D treatment in MH-S cells with or without *Ythdf2* silencing. (M) Hmox1 and Ythdf2 protein levels, (N) and mRNA levels in *Ythdf2*-overexpression adenovirus infected MH-S cells. For A-I, n = 8 mice per group. For J-N, results are representative of 3 separate experiments. The data are shown as mean ± SE; $^{*}P < 0.05$, $^{**}P < 0.01$, $^{***}P < 0.001$, $^{\$\$}P < 0.01$, $^{\$\$\$}P < 0.001$ vs WT (NRX) or shCon or Vector group; $^{\#}P < 0.05$, $^{\#\#\#}P < 0.001$ vs WT (HPX) group. AMs = alveolar macrophages; BALF = bronchoalveolar lavage fluid; SOD = superoxide dismutase; GSH = glutathione; T-AOC = total antioxidant capacity; MDA = malondialdehyde; NRX = normoxia; HPX = hypoxia; WT=$Ythdf2^{wildtype}$; KO=$Ythdf2^{Lyz2\ Cre}$.

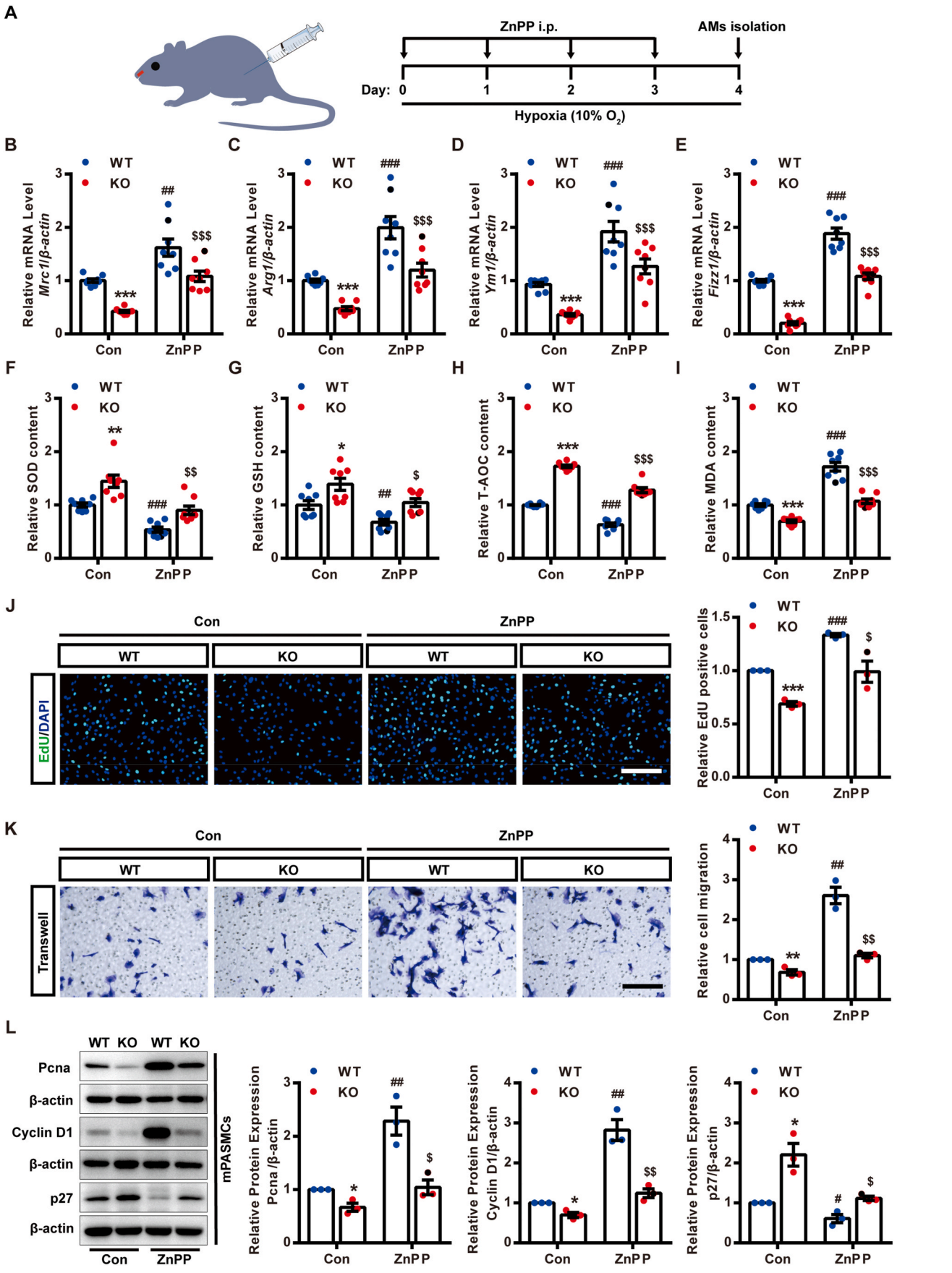

(caption on next page)

Fig. 6. Pharmacological blockade of *Hmox1* rescues the anti-inflammatory and anti-oxidant effects of *Ythdf2* deficiency in alveolar macrophages. (A) Schematic representation of AMs isolation from mice exposed to hypoxia with ZnPP treatment. (B) *Mrc1*, (C)Arg*1*, (D)*Ym1* and (E) *Fizz1* mRNA levels in AMs from WT and KO mice with or without ZnPP treatment under hypoxia treated for 4 days. (F–I) The content of (F) SOD, (G) GSH, (H) T-AOC, and (I) MDA in AMs from WT and KO mice exposed to hypoxia for 4 days with or without ZnPP treatment. In B–I, n = 8 mice per group. (J) EdU (green) staining, (K) Transwell assay, (L) and immunoblotting of Pcna, Cyclin D1 and p27 in mPASMCs exposed to conditioned media from AMs of WT and KO mice exposed to hypoxia for 4 days with or without ZnPP treatment. For J-K, scale bars = 200 μm, for J-L, results are representative of 3 separate experiments. The data are shown as mean ± SE; *P < 0.05, **P < 0.01, ***P < 0.001, $^{\#}$P < 0.05, $^{\#\#}$P < 0.01, $^{\#\#\#}$P < 0.001 vs WT (Con) group; $^{\$}$P < 0.05, $^{\$\$}$P < 0.01, $^{\$\$\$}$P < 0.001 vs KO (Con) group. AMs = alveolar macrophages; ZnPP = Zinc Protoporphyrin; SOD = superoxide dismutase, GSH = glutathione, T-AOC = total antioxidant capacity, MDA = malondialdehyde; WT=*Ythdf2*^{wildtype}; KO=*Ythdf2*$^{Lyz2\ Cre}$; mPASMCs = mouse pulmonary artery smooth muscle cells. (For interpretation of the references to colour in this figure legend, the reader is referred to the Web version of this article.)

results suggested that *Ythdf2* mediated inflammation and oxidation of AMs by degrading *Hmox1* mRNA in the pathogenesis of PH.

3.6. *Hmox1* inhibition eliminates the anti-inflammatory and anti-oxidant effects in *Ythdf2* $^{Lyz2\ cre}$ mice under hypoxic exposure

To determine whether the early decrease of *Hmox1* expression mediated by *Ythdf2* is essential for the later development of PH, we next evaluated whether pharmacological blockade of *Hmox1* with ZnPP could eliminate the anti-inflammatory and anti-oxidant effects of *Ythdf2* deficiency in AMs (Fig. 6A). As expected, ZnPP treatment inhibited *Hmox1* expression induced by *Ythdf2* deficiency and further aggravated inflammation, oxidative stress, and PASMCs proliferation in *Ythdf2*$^{wild\text{-}type}$ mice under hypoxic condition (Fig. S8A and Fig. 6B–L). Myeloid *Ythdf2* deficiency decreased the expression of M2 markers in AMs after hypoxia for 4 days, and this decrease could be totally reversed by ZnPP treatment (Fig. 6B–E). Meanwhile, in the lungs of ZnPP treated-*Ythdf2*$^{Lyz2\ Cre}$ mice under hypoxic exposure for 4 days, the mRNA levels of *Il6* and *Ccl2* were also significantly higher than those without ZnPP treatment (Figs. S9A and B). These results suggested that *Hmox1* inhibition can polarize the population of AMs toward the M2 phenotype under hypoxic conditions.

In addition, the *Il10* expression level and anti-oxidant effects were increased in AMs from hypoxic *Ythdf2*$^{Lyz2\ Cre}$ mice as compared to *Ythdf2*^{wildtype} mice, which were substantially blocked by ZnPP treatment (Fig. S9C and Fig. 6F–I). These findings demonstrated that *Hmox1* inhibition shifts the phenotype of AMs in *Ythdf2* deficient mice from an anti-inflammatory and anti-oxidant to a pro-inflammatory and pro-oxidative phenotype. Given the altered phenotype of AMs in ZnPP treated *Ythdf2*$^{Lyz2\ Cre}$ mice, we incubated mPASMCs with CM of AMs from *Ythdf2*^{wildtype} mice and *Ythdf2*$^{Lyz2\ Cre}$ mice (with or without ZnPP treatment) exposed to hypoxia for 4 days. As shown by EdU assay, transwell assay and WB, CM from *Ythdf2* deficient AMs induced decreases in proliferation and migration of PASMCs, whereas these effects were almost blocked by ZnPP treatment (Fig. 6J-L). Therefore, the above observations demonstrated that *Hmox1* inhibition can block the anti-inflammatory and anti-oxidant effects of *Ythdf2* deficiency *in vitro*.

3.7. The protective role of myeloid Ythdf2 deficiency in PH mice is reversed by ZnPP treatment

Early macrophage activation is critical for the later progression of PH, we next evaluated whether *Hmox1* inhibition can deteriorate the progression of PH in *Ythdf2*$^{Lyz2\ Cre}$ mice undergo Su/Hx exposure *in vivo*. ZnPP was injected to *Ythdf2*^{wildtype} mice and *Ythdf2* $^{Lyz2\ Cre}$ mice on days 0, 1, 2, 3, 7, 14, and 21 post-Su/Hx exposure, and the assessment of PH parameters was performed after Su/Hx treated for 4 weeks (Fig. 7A). Genetic ablation of *Ythdf2* in myeloid cells alleviated the increase of RVSP and RV/(LV + S) induced by Su/Hx treatment, while ZnPP exposure reversed this protective role (Fig. 7B and C). Echocardiography also revealed that myeloid specific *Ythdf2* deficiency induced improvement of VTI and PAT/PET in Su/Hx PH mice were abrogated by ZnPP treatment (Fig. 7D). Increased medial thickness and muscularization of the distal pulmonary artery wall were also found in ZnPP treated *Ythdf2*$^{Lyz2\ Cre}$ mice under Su/Hx exposure (Fig. 7E). In contrast with decreased M2 polarization in Su/Hx mice with myeloid *Ythdf2* deficiency, ZnPP treatment induced a marked increase in *Mrc1* positive macrophages in lung sections of Su/Hx treated *Ythdf2*$^{Lyz2\ Cre}$ mice (Fig. S10A). Meanwhile, IF staining also revealed that ZnPP treatment showed an increased number of Pcna stained cells in Su/Hx treated *Ythdf2*$^{Lyz2\ Cre}$ mice (Fig. S10B). Similarly, the decreased expression of inflammatory factors and cytokines including *Il6*, *transforming growth factor beta (Tgfβ)* and *platelet derived growth factor (Pdgf)* in hypoxic *Ythdf2*$^{Lyz2\ Cre}$ mice were also reversed by ZnPP treatment (Figs. S11A–C). Overall, our data suggest that *Hmox1* is necessary for attenuating macrophage activation and improving PVR in myeloid *Ythdf2* deficiency mice under Su/Hx exposure.

4. Discussion

PH is a serious cardiorespiratory disorder associated with irreversible arteriolar vessel occlusion and increased pulmonary arterial pressure (PAP). The accumulation and activation of monocytes and macrophages in perivascular and adventitial space is a major characteristic of PH. The vascular inflammation is tightly correlated with vascular remodeling and mean PAP [9,33]. However, no satisfactory treatment for PH perivascular inflammation is available up to now. Thus, screening for new macrophage targets may be a promising approach to treat pulmonary inflammation and PH. Although m^{6}A modification and *Ythdf2* have been reported to be involved in the development of PH, the molecular mechanism of *Ythdf2* in PH pathogenesis is poorly understood. More importantly, whether *Ythdf2* could regulate macrophage oxidative stress and inflammation and thus participate in PH development remain to be further studied. Here, we first report the RBPs of m^{6}A modification, Ythdf2, was involved in vascular inflammation and pathological remodeling in the pathogenesis of PH. Specific disruption of *Ythdf2* in macrophages by genetic approaches alleviated alternative activation of macrophages and PASMCs proliferation *in vivo* and *in vitro*. *Hmox1* was identified as a potential target of *Ythdf2* by proteomics, MeRIP and Ythdf2-RIP assays. Mechanistically, *Ythdf2* can promote *Hmox1* mRNA degradation in an m^{6}A dependent manner in pulmonary macrophages. In addition, *Hmox1* inhibition abrogated the protective role of myeloid *Ythdf2* deficiency in PH mice. Overall, from the perspective of the reader, the present study suggests that *Ythdf2* may be a potential therapeutic target for vascular inflammation and PVR in PH.

The preponderance of evidence shows pro-fibrotic and proliferative M2 macrophages contribute to the pathogenesis of PH [13,44]. During the progression of PH, M2 macrophage polarization is induced in the early period of hypoxia, while *Ythdf2* has been previously reported to regulate macrophage polarization. In this study, significant enrichment of *Ythdf2* in pulmonary macrophages was detected in human PAH patients and experimental PH models. Importantly, as early as 4 days after hypoxia, Ythdf2 protein expression in AMs peaked while remained elevated for at least 28 days after Su/Hx treated. Similarly, Ythdf2 protein expression in lungs of Su/Hx treated mice also showed a significant increase in the earlier period of PH while gradually decreased during PH development. These results suggest that there are signals in lungs or AMs that can greatly up-regulate Ythdf2 protein expression early on after hypoxic exposure, but the expression of Ythdf2 may still be

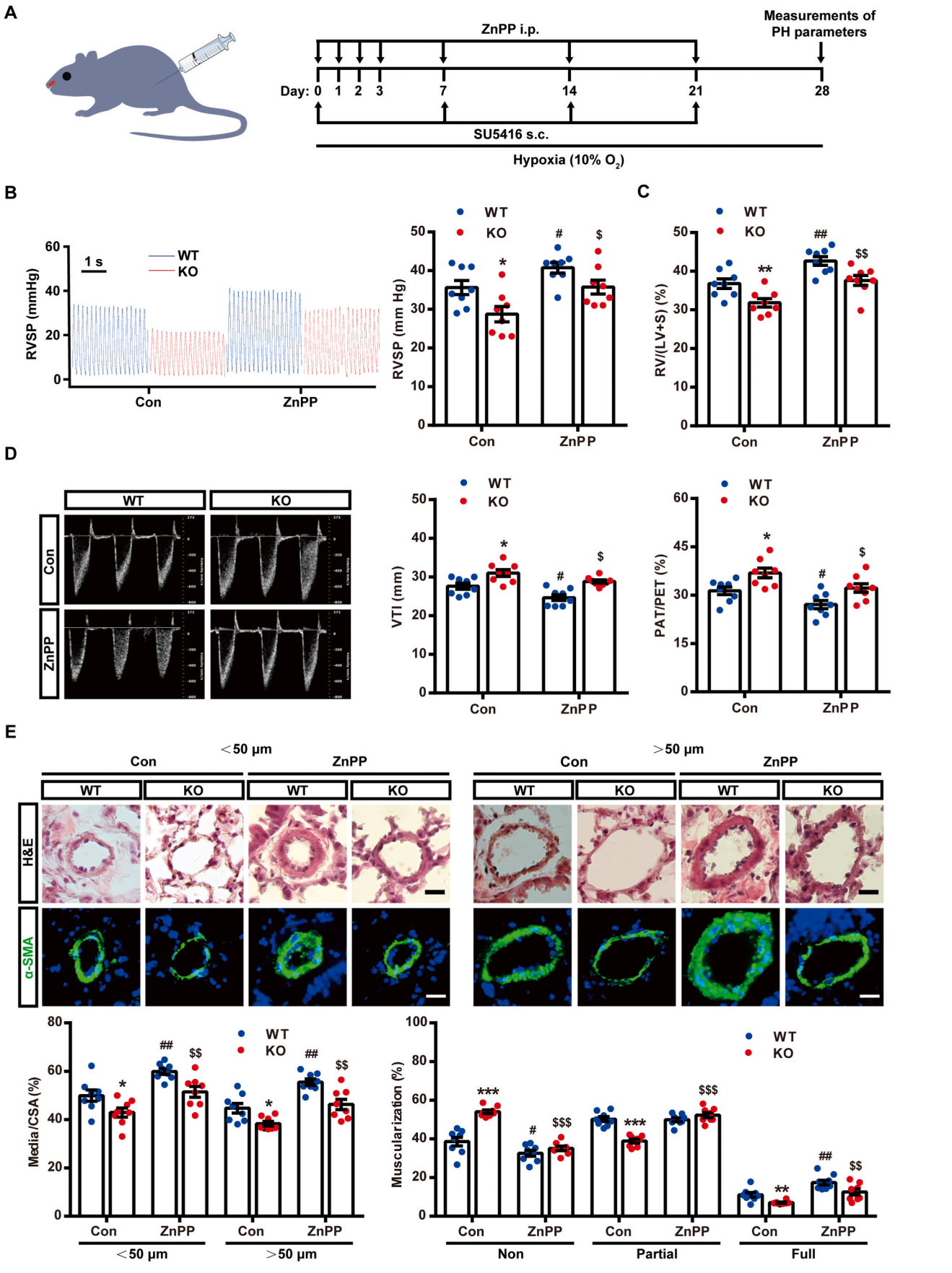

(caption on next page)

Fig. 7. The protective effect of *Ythdf2* myeloid deficiency against PH was abrogated by ZnPP treatment in mice. (A) Schematic presentation of experimental protocol for the treatment of WT and KO mice with ZnPP in the Su/Hx-induced PH model. (B) Right ventricular systolic pressure, (C) changes in the right ventricular structure shown as the ratio of the right ventricular (RV) and the left ventricular plus septum (LV + septum) mass, (D) echocardiographic assessment of right ventricular systolic function depicted by velocity time integral (VTI), and the ratio of pulmonary artery accelerate time to ejection time (PAT/PET), in WT and KO mice under Su/Hx exposure with or without ZnPP treatment. (E) Representative images of H&E staining and α-SMA (green) immunohistochemical staining of the distal pulmonary arteries, quantification of medial wall thickness index, and proportion of non, partially, or fully muscularized pulmonary arteries are shown, scale bars = 20 μm. The data are shown as mean ± SE, and n = 8 mice per group; *P < 0.05, **P < 0.01, ***P < 0.001, $^{\#}$P < 0.05, $^{\#\#}$P < 0.01 vs WT (Con) group; $^{\$}$P < 0.05, $^{\$\$}$P < 0.01, $^{\$\$\$}$P < 0.001 vs KO (Con) group. Su/Hx = SU5416/hypoxia; WT=*Ythdf2*^{wildtype}; KO=*Ythdf2*$^{Lyz2\ Cre}$; ZnPP = Zinc Protoporphyrin. (For interpretation of the references to colour in this figure legend, the reader is referred to the Web version of this article.)

responsive to some potential secondary signals that are likely to be compensatory in nature. Interestingly, several posttranslational modifications have been reported to regulate the expression of *Ythdf2* in recent years [45–47], which may contribute to this process. It will be important for future studies to identify how hypoxia or Su/Hx treatments result in such pattern of regulation of Ythdf2 protein expression in lungs or AMs. Reduced expression of M2 markers and inflammatory factors were also observed in AMs from myeloid *Ythdf2* deficient mice after hypoxia for 4 days. Accumulating evidence suggest that the switch in macrophage phenotype occurred within the first 4 days of hypoxia [3,13]. To the best of our knowledge, this is the first study to propose a link between the Ythdf2 protein expression and early alternative activation of macrophages in PH.

Early M2 polarization is critical for later vascular remodeling in the development of PH [13]. These polarized trophic macrophages secrete much inflammatory factors, cytokines and other pro-mitogenic factors, thus promoting PASMCs proliferation and resulting in PVR. Recently, *Fizz1* overexpression has been reported to cause PH due to its mitogenic, vasoconstrictive and angiogenic properties [13,48]. Elevated expression of Arg*1* is also associated with PH severity [36,49]. In agreement with these, our findings also demonstrated improved hemodynamic parameters and pathological remodeling of Su/Hx-induced mice in the absence of *Ythdf2*. As a result, fewer proliferation was also observed in PASMCs after incubating with CM from AMs in hypoxic myeloid *Ythdf2* deficient mice.

In hypoxic AMs with *Ythdf2* deficiency, elevated levels of Hmox1 protein were detected by omics analysis. *Ythdf2* can recognize and facilitate m^{6}A modified mRNA degradation. Consistently, we found that downregulation of *Hmox1* is accompanied with the upregulation of Ythdf2 protein in AMs of PH. MeRIP and *Ythdf2*-RIP assays also confirmed that *Hmox1* is a downstream target for *Ythdf2* in pulmonary macrophages. *Hmox1* has been reported to suppress macrophage accumulation, M2 activation and cytokine production in BALF and attenuate the subsequent progression of PH [13]. CO is the key catalytic product of *Hmox1*, which have potent anti-inflammatory role through promoting the expression of *Il10* [50,51]. Decreased expression of M2 markers and increased levels of *Il10* were also observed in AMs from hypoxic *Ythdf2*$^{Lyz2\ cre}$ mice, which is in agreement with the previous studies.

Additionally, in PASMCs co-cultured with CM from AMs after hypoxia for 4 days, the supernatant of AMs with *Ythdf2* inhibition alleviated the proliferation of mPASMCs. Of which, reduced secretion of cytokines, inflammatory factors and M2 markers in *Ythdf2* deficient AMs may be the major contributing factor. However, *Hmox1* is also reported to inhibit VSMCs proliferation in arterial remodeling [52]. It is also possible that the increased secretion of Hmox1 was uptake by PASMCs, and then exert an anti-proliferative role in PASMCs. Thus, the underlying mechanism of PASMCs proliferation in co-culture system may need to be further clarified.

In a previous study, *Hmox1* in rat lungs is upregulated after hypoxia only for 9 h, which was considered as a compensatory mechanism induced by hypoxia [53]. Correspondingly, we found that Hmox1 was downregulated in AMs at the first day of hypoxia. *Hmox1* inhibition have been shown to promote atherosclerosis, which correlated with increased ROS generation and greater release of inflammatory cytokines, including *Il6* and *Ccl2* [38]. Similarly, reversed M2 polarization and improved oxidative state were found in AMs from hypoxic *Ythdf2*$^{Lyz2\ cre}$ mice, and *Hmox1* inhibition can eliminate the protective role induced by *Ythdf2* deficiency. These results support the hypothesis that *Hmox1* can act as a pivot to shift the balance of immune response from proinflammatory toward immunosuppressive in this critical period due to its anti-inflammatory and antioxidant roles in immunomodulation. Moreover, ZnPP treatment inhibited the expression of *Hmox1* and accelerated the development of PH in Su/Hx treated *Ythdf2*$^{Lyz2\ cre}$ mice. It is consistent with a previous study showing that more sustained increases in *Hmox1* expression are protective in PH [13]. However, it should be noted that ZnPP, as a potent selective inhibitor of HO (including but not limited to *Hmox1*), has also been shown to inhibit soluble guanylyl cyclase and NOS [54], thus here the possibility of non-specific ZnPP actions can not be excluded completely in this study.

In summary, for the first time, we demonstrate a link between *Ythdf2*

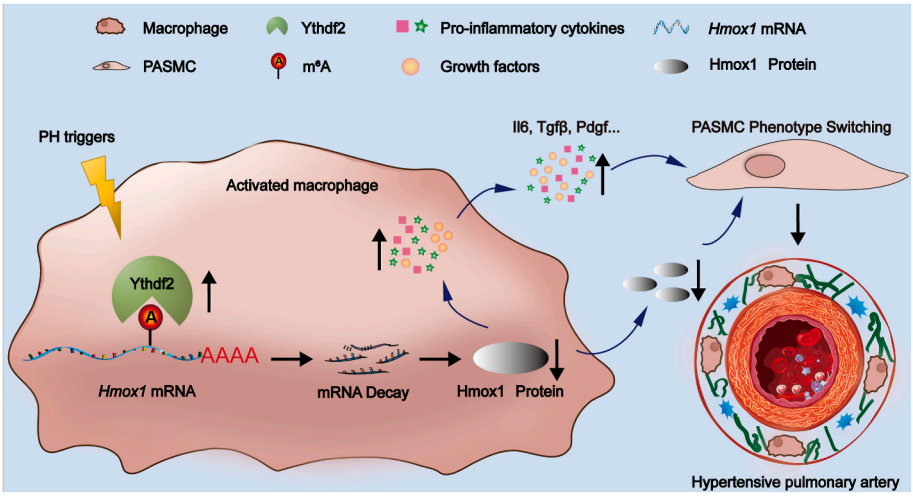

Fig. 8. A schematic diagram indicates the mechanisms of how *Ythdf2* in macrophages promote pulmonary vascular remodeling during PH pathogenesis.

and early alternative activation of macrophages and the pathogenesis of PH. M^6A modification and Ythdf2 recognition were identified on *Hmox1* mRNA in AMs during the development of PH. *Ythdf2* can facilitate M2 polarization, vascular inflammation and oxidative stress at the early stage of PH by degrading the *Hmox1* mRNA. Myeloid *Ythdf2* deficiency protects mice against Su/Hx induced-PH, and this protective role is eliminated by *Hmox1* inhibition (Fig. 8). On the basis of our findings, *Ythdf2* may be a potential target for M2 activation and PVR in PH diagnosis or therapeutic treatment.

Author contributions

FC, JW, LH and YFY designed the research and wrote the manuscript; LH, JW, YFY, YYS, HJH and DHL performed the experiments; LH, JW, YFY, KW, YJY, KL and YC analyzed data; QW, XXS, ZBQ, DW, BS, JYC, DF and YJ provided human patient samples, performed the animal model, and performed critical reading/editing of the manuscript; FC and LH supervised the study.

Funding

This work was supported by the National Natural Science Foundation of China grants (No.82225023, No.82200057, No.82121001, No.81922041 and No.81772020), the Natural science research project of Jiangsu higher education institutions grant BK20220321 and 18KJB340002, the China Postdoctoral Science Foundation (2021M701758), and the Postdoctoral Research Project of Gusu School of Nanjing Medical University (GSBSHKY202103).

Declaration of competing interest

The authors declare that they have no known competing financial interests or personal relationships that could have appeared to influence the work reported in this paper.

Data availability

Data will be made available on request.

Appendix A. Supplementary data

Supplementary data to this article can be found online at https://doi.org/10.1016/j.redox.2023.102638.

References

[1] P.M. Hassoun, Pulmonary arterial hypertension, N. Engl. J. Med. 385 (25) (2021) 2361–2376.
[2] N.F. Ruopp, B.A. Cockrill, Diagnosis and treatment of pulmonary arterial hypertension: a review, JAMA 327 (14) (2022) 1379–1391.
[3] T. Hashimoto-Kataoka, et al., Interleukin-6/interleukin-21 signaling axis is critical in the pathogenesis of pulmonary arterial hypertension, Proc. Natl. Acad. Sci. U. S. A. 112 (20) (2015) E2677–E2686.
[4] M.R. Nicolls, N.F. Voelkel, The roles of immunity in the prevention and evolution of pulmonary arterial hypertension, Am. J. Respir. Crit. Care Med. 195 (10) (2017) 1292–1299.
[5] M. Rabinovitch, et al., Inflammation and immunity in the pathogenesis of pulmonary arterial hypertension, Circ. Res. 115 (1) (2014) 165–175.
[6] A. Huertas, et al., Chronic inflammation within the vascular wall in pulmonary arterial hypertension: more than a spectator, Cardiovasc. Res. 116 (5) (2020) 885–893.
[7] L. Wang, et al., Mice with a specific deficiency of Pfkfb3 in myeloid cells are protected from hypoxia-induced pulmonary hypertension, Br. J. Pharmacol. 178 (5) (2021) 1055–1072.
[8] A. Ntokou, et al., Macrophage-derived PDGF-B induces muscularization in murine and human pulmonary hypertension, JCI Insight 6 (6) (2021).
[9] M. Sahara, et al., Diverse contribution of bone marrow-derived cells to vascular remodeling associated with pulmonary arterial hypertension and arterial neointimal formation, Circulation 115 (4) (2007) 509–517.
[10] M.G. Frid, et al., Hypoxia-induced pulmonary vascular remodeling requires recruitment of circulating mesenchymal precursors of a monocyte/macrophage lineage, Am. J. Pathol. 168 (2) (2006) 659–669.
[11] D.M. Mosser, J.P. Edwards, Exploring the full spectrum of macrophage activation, Nat. Rev. Immunol. 8 (12) (2008) 958–969.
[12] X. Mao, et al., Single-cell RNA-sequencing reveals the active involvement of macrophage polarizations in pulmonary hypertension, Dis. Markers 2022 (2022), 5398157.
[13] E. Vergadi, et al., Early macrophage recruitment and alternative activation are critical for the later development of hypoxia-induced pulmonary hypertension, Circulation 123 (18) (2011) 1986–1995.
[14] A. Yaku, et al., Regnase-1 prevents pulmonary arterial hypertension through mRNA degradation of interleukin-6 and platelet-derived growth factor in alveolar macrophages, Circulation 146 (13) (2022) 1006–1022.
[15] T. Thenappan, et al., Pulmonary arterial hypertension: pathogenesis and clinical management, BMJ 360 (2018) j5492.
[16] L. Hu, et al., YTHDF1 regulates pulmonary hypertension through translational control of MAGED1, Am. J. Respir. Crit. Care Med. 203 (9) (2021) 1158–1172.
[17] X. Wang, C. He, Reading RNA methylation codes through methyl-specific binding proteins, RNA Biol. 11 (6) (2014) 669–672.
[18] U. Sheth, R. Parker, Decapping and decay of messenger RNA occur in cytoplasmic processing bodies, Science 300 (5620) (2003) 805–808.
[19] Y. Qin, et al., The m(6)A methyltransferase METTL3 promotes hypoxic pulmonary arterial hypertension, Life Sci. 274 (2021), 119366.
[20] P. Liu, et al., m(6)A modification-mediated GRAP regulates vascular remodeling in hypoxic pulmonary hypertension, Am. J. Respir. Cell Mol. Biol. 67 (5) (2022) 574–588.
[21] X. Gu, et al., N6-methyladenosine demethylase FTO promotes M1 and M2 macrophage activation, Cell. Signal. 69 (2020), 109553.
[22] L. Cai, et al., YTHDF2 regulates macrophage polarization through NF-kappaB and MAPK signaling pathway inhibition or p53 degradation, Dis. Markers 2022 (2022), 3153362.
[23] G. Su, et al., YTHDF2 is a potential biomarker and associated with immune infiltration in kidney renal clear cell carcinoma, Front. Pharmacol. 12 (2021), 709548.
[24] W. Liu, et al., Pan-cancer analysis identifies YTHDF2 as an immunotherapeutic and prognostic biomarker, Front. Cell Dev. Biol. 10 (2022), 954214.
[25] M. Qi, et al., m(6) A reader protein YTHDF2 regulates spermatogenesis by timely clearance of phase-specific transcripts, Cell Prolif 55 (1) (2022), e13164.
[26] S.H. Kim, et al., Reprograming of tumor-associated macrophages in breast tumor-bearing mice under chemotherapy by targeting heme oxygenase-1, Antioxidants 10 (3) (2021).
[27] Z. Tang, et al., HO-1-mediated ferroptosis as a target for protection against retinal pigment epithelium degeneration, Redox Biol. 43 (2021), 101971.
[28] J. Wang, et al., CAR (CARSKNKDC) peptide modified ReNcell-derived extracellular vesicles as a novel therapeutic agent for targeted pulmonary hypertension therapy, Hypertension 76 (4) (2020) 1147–1160.
[29] L. Hu, et al., Mesenchymal stem cell-derived nanovesicles as a credible agent for therapy of pulmonary hypertension, Am. J. Respir. Cell Mol. Biol. 67 (1) (2022) 61–75.
[30] Y. Zhou, et al., SRAMP: prediction of mammalian N6-methyladenosine (m6A) sites based on sequence-derived features, Nucleic Acids Res. 44 (10) (2016) e91.
[31] X. Luo, et al., RMVar: an updated database of functional variants involved in RNA modifications, Nucleic Acids Res. 49 (D1) (2021) D1405–D1412.
[32] A. Hoshino, et al., Extracellular vesicle and particle biomarkers define multiple human cancers, Cell 182 (4) (2020) 1044–1061 e18.
[33] M.K. Steiner, et al., Interleukin-6 overexpression induces pulmonary hypertension, Circ. Res. 104 (2) (2009) 236–244, 28pp. following 244.
[34] O. Sanchez, et al., Role of endothelium-derived CC chemokine ligand 2 in idiopathic pulmonary arterial hypertension, Am. J. Respir. Crit. Care Med. 176 (10) (2007) 1041–1047.
[35] E. Daley, et al., Pulmonary arterial remodeling induced by a Th2 immune response, J. Exp. Med. 205 (2) (2008) 361–372.
[36] Y. Jin, et al., Mice deficient in Mkp-1 develop more severe pulmonary hypertension and greater lung protein levels of arginase in response to chronic hypoxia, Am. J. Physiol. Heart Circ. Physiol. 298 (5) (2010) H1518–H1528.
[37] K. Yamaji-Kegan, et al., Hypoxia-induced mitogenic factor has proangiogenic and proinflammatory effects in the lung via VEGF and VEGF receptor-2, Am. J. Physiol. Lung Cell Mol. Physiol. 291 (6) (2006) L1159–L1168.
[38] L.D. Orozco, et al., Heme oxygenase-1 expression in macrophages plays a beneficial role in atherosclerosis, Circ. Res. 100 (12) (2007) 1703–1711.
[39] S.H. Vitali, et al., Divergent cardiopulmonary actions of heme oxygenase enzymatic products in chronic hypoxia, PLoS One 4 (6) (2009) e5978.
[40] D. Willis, et al., Heme oxygenase: a novel target for the modulation of the inflammatory response, Nat. Med. 2 (1) (1996) 87–90.
[41] A. Belhaj, et al., Heme oxygenase-1 and inflammation in experimental right ventricular failure on prolonged overcirculation-induced pulmonary hypertension, PLoS One 8 (7) (2013), e69470.
[42] A. Katseff, R. Alhawaj, M.S. Wolin, Redox and inflammatory signaling, the unfolded protein response, and the pathogenesis of pulmonary hypertension, Adv. Exp. Med. Biol. 1304 (2021) 333–373.
[43] T. Minamino, et al., Targeted expression of heme oxygenase-1 prevents the pulmonary inflammatory and vascular responses to hypoxia, Proc. Natl. Acad. Sci. U. S. A. 98 (15) (2001) 8798–8803.
[44] A.L. Mora, et al., Activation of alveolar macrophages via the alternative pathway in herpesvirus-induced lung fibrosis, Am. J. Respir. Cell Mol. Biol. 35 (4) (2006) 466–473.

[45] G. Hou, et al., SUMOylation of YTHDF2 promotes mRNA degradation and cancer progression by increasing its binding affinity with m6A-modified mRNAs, Nucleic Acids Res. 49 (5) (2021) 2859–2877.
[46] R. Fang, et al., EGFR/SRC/ERK-stabilized YTHDF2 promotes cholesterol dysregulation and invasive growth of glioblastoma, Nat. Commun. 12 (1) (2021) 177.
[47] J. Yu, et al., Histone lactylation drives oncogenesis by facilitating m(6)A reader protein YTHDF2 expression in ocular melanoma, Genome Biol. 22 (1) (2021) 85.
[48] X. Teng, et al., FIZZ1/RELMalpha, a novel hypoxia-induced mitogenic factor in lung with vasoconstrictive and angiogenic properties, Circ. Res. 92 (10) (2003) 1065–1067.
[49] W. Durante, et al., Transforming growth factor-beta(1) stimulates L-arginine transport and metabolism in vascular smooth muscle cells: role in polyamine and collagen synthesis, Circulation 103 (8) (2001) 1121–1127.
[50] T. Dolinay, et al., Inhaled carbon monoxide confers antiinflammatory effects against ventilator-induced lung injury, Am. J. Respir. Crit. Care Med. 170 (6) (2004) 613–620.
[51] S. Inoue, et al., Transfer of heme oxygenase 1 cDNA by a replication-deficient adenovirus enhances interleukin 10 production from alveolar macrophages that attenuates lipopolysaccharide-induced acute lung injury in mice, Hum. Gene Ther. 12 (8) (2001) 967–979.
[52] H.J. Duckers, et al., Heme oxygenase-1 protects against vascular constriction and proliferation, Nat. Med. 7 (6) (2001) 693–698.
[53] H. Christou, et al., Prevention of hypoxia-induced pulmonary hypertension by enhancement of endogenous heme oxygenase-1 in the rat, Circ. Res. 86 (12) (2000) 1224–1229.
[54] S.D. Appleton, et al., Selective inhibition of heme oxygenase, without inhibition of nitric oxide synthase or soluble guanylyl cyclase, by metalloporphyrins at low concentrations, Drug Metab. Dispos. 27 (10) (1999) 1214–1219.